ON-BOARD IMAGES TO SPECIFY AND COMMISSION THE ADCS

Boris Segret [1], Sam Bammens [2], Sergio Bras [2], Dominik Marszk [2], Vasundhara Shiradhonkar [2], Vladimir Zelenevskiy [2], David Evans [2]

[1] *CENSUS, Paris Observatory – PSL, 5, pl. Jules Janssen – 92195 Meudon Cedex, France, +33 1 45 07 78 24, Boris.Segret@observatoiredeparis.psl.eu*
[2] *ESOC, European Space Agency, Robert-Bosch-Str. 5, 64293 Darmstadt, Germany, +49 6151 90 2000, David.Evans@esa.int*

Abstract

ADCS for nanosatellites in the New Space sector are frequently offered as Commercial-Off-The-Shelves (COTS) systems. However, when the COTS datasheet and the actual performance in flight differ dramatically, there are few means to assess the discrepancies. Here, we report on the operations with a flying nanosatellite to assess the attitude stability during inertial pointing mode, based on the analysis of on-board images of the sky. The satellite is OPS-SAT, a 3-unit CubeSat owned and operated by ESA. The imager is directed to the -Z longitudinal axis. After a trial and error process, a set up to capture 5 images in a row of the dark sky was adopted and run multiple times. A complex processing revealed that many stars could also be identified. It demonstrates that the pointing did not reach the requested performance and, moreover, it provides a fine assessment of the actual pointing and its jitter and drift. This information was fundamental in assessing the effectiveness of modifications that were introduced into the operations and the on-board systems. The new images showed the improvements in both the absolute pointing and the attitude knowledge. Such assessments were possible with a small optical sensor and despite the light of stars is spread over tens of pixels. Yet, the processing is still complex, but the lessons learned are helpful to specify requirements and tests for future COTS, as well as a commissioning process in flight.

1   INTRODUCTION

Originally, we presented an astrometry experiment to fly on OPS-SAT. Due to some known issues with inertial pointing, we decided to first image stars and assess the feasibility of the experiment. While the OPS-SAT team (at ESA) tested operations to stabilize the inertial pointing, took sky pictures from the orbit and downloaded them, the CENSUS team (at Paris Observatory – PSL) was in charge of processing the pictures to assess the actual pointing of the platform. It took about 3 weeks to see stars in the images and to get a characterization of the field of view: the problem was the density of cosmic rays.

Then, the process was consolidated, and the operations were set up to take 5 images in a row. We gathered a large dataset of pictures in various conditions of stray light and stability. We could stack some of the sets of 5 images-in-a-row and detect even more stars. After cleaning and stacking, we
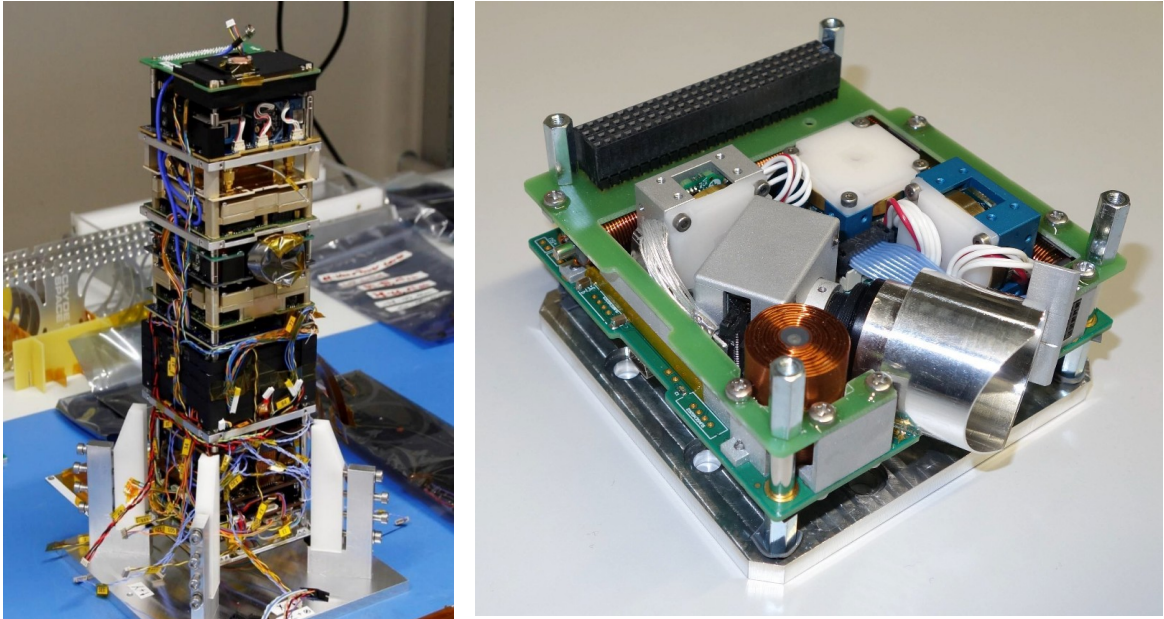
Figure 1: ESA's OPS-SAT (left) launched on 18th Dec 2019 and its iADCS-100 before integration (right) that is also visible on the main picture in the middle of the stack. Credit ESA.

could match some stacked images with regions of the sky. From these characterizations, it became clear that the pointing was erratic, as well as being unstable.

The operations and ADCS configuration were adapted further and, at some point, we could get a few matches on the sky that were close to the requested quaternions. A careful analysis compared the fields of view as requested during mission preparation, as recognized from the images and as on-board estimated. The work is still in progress and suggests that an update of the alignment quaternions used on board for the various sensors is possible.

2   EXPERIMENT on OPS-SAT

2.1   OPS-SAT hardware

OPS-SAT (Fig. 1), also called by ESA "the flying software lab", is a 3-Unit CubeSat (main body within 30 cm × 10 cm × 10 cm) and the first nanosatellite directly owned by ESA and controlled by ESA/ESOC in Darmstadt, Germany [1], [2]. It flies in low Earth orbit, on a polar 6:00-18:00 Sun-synchronous orbit. It is equipped with a full set of sensors and actuators, in particular the imager IMS-100 by Berlin Space Technologies GmbH (BST) and two Attitude Determination and Control Systems (ADCS), the "cADCS" as a course-pointing system using a fine sun sensor, photo diodes, gyros and magnetometers as sensors, but no star tracker, and the "iADCS-100" by BST as a fine-guidance ADCS that includes a star tracker. The bus is based on the NanoMind on-board computers by GOMSPACE running flight software developed by GMV Poland. The system prime and integrator is TU Graz of Austria. The main solar panels, once deployed, consist of five strings of 30 cm × 10 cm normal to - X axis. OPS-SAT offers a high datalink in S-band and X-band to download and check on ground the results of the on-board experiments.

The imager is aligned with the satellite's longitudinal axis, directed to -Z (Fig. 2). The iADCS star tracker points in the satellite's transversal plane, to the (+X,-Y) quarter. According to private communications with a star tracker manufacturer for CubeSats, the Attitude Knowledge Error (AKE) can be expected to be within 15 arcsec transversely to its line of sight, but it likely increases by a factor of 5 to 6 for the axis rotation error. For OPS-SAT, whose imager is not aligned with the
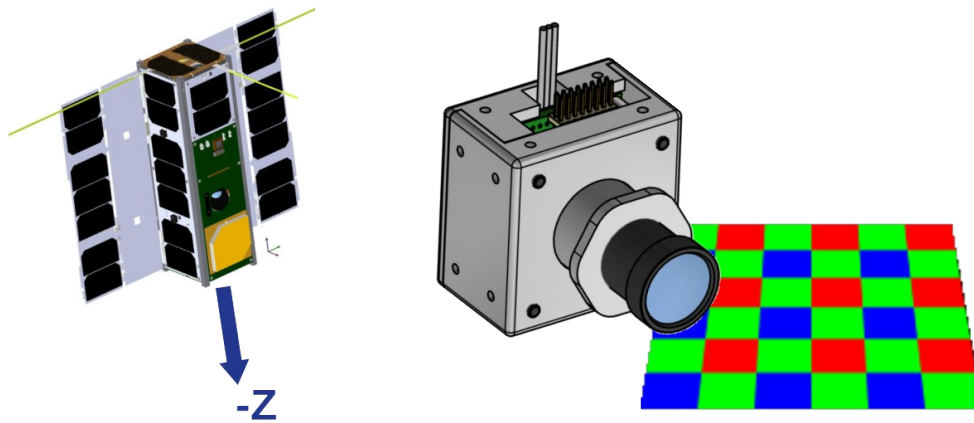
Figure 2: IMS-100 with an RGGB Bayer pattern, directed to OPS-SAT's -Z axis

star tracker, the start tracker's AKE to be considered in the IMS-100 field of view is likely not isotrope and could reach up to 90 arcsec (not considering estimation filters that are embedded in the ADCS).

The IMS-100 is a converted COTS star tracker that was modified to image the Earth surface. Hence, the calibration and acceptance tests for this device addressed rather the risk of image distortion and not explicitly the sensitivity. The raw images are coded in the IMS-100 on 12 bits per pixel, using an RGGB Bayer pattern, on a 2048 × 1944 matrix of pixels covering approximately a 10° × 10° field of view, with pixels of ~18 arcsec. They can be converted on board in 3-color 8 bit PNG format with debayering, or deliver in raw format without debayering. The properties at imaging stars were unknown at the time of our experiment.

OPS-SAT allows to fly algorithms directly written for Linux shell, in JAVA, Python or C++. To this aim, the Institute of Communication Networks and Satellite Communications, from Graz University of Technology, Austria, developed a system on module called the Satellite Experimental Processing Platform (SEPP), with a library of high-level functions to interface with various OPS-SAT systems, like the imager and the iADCS. Hence, the experimenter's code can use functions of SEPP only rather than any functions of the sensors' and actuators' interfaces directly. SEPP is of great help for the experimenter who, nevertheless, still needs to understand and care of the correct chronology in the activation of OPS-SAT's systems and of their detailed status before proceeding from one step to the next. A full framework in Eclipse IDE was prepared to cross-compile the experiment code from the experimenter's environment (Intel, AMD) to the target environment, namely OPS-SAT with an ARM processor.

An "experimenter" can be any kind of team from Europe industry or academia, whose idea is deemed feasible and relevant with OPS-SAT operations. There have been over 200 experiments registered in early 2022. The experiments are pieces of software or firmware to be run on board OPS-SAT, under the principle of "develop, fly, improve" cycles. When the experiment is ready, a test on the flatsat is performed. Then, the orbital deployment is decided (uploading the software and planning its execution) and a validation report terminates the cycle, to assess if debugging is required or new orbital deployment are needed.

OPS-SAT is operational since mid-2020. During the commissioning, various iADCS pointing modes were tested with varying degrees of success. An issue was identified with an unstable behavior during inertial pointing. The star tracker does not always provide quaternions when requested, due to possible illumination. Due to magnetic interaction between the reaction wheels and the iADCS magnetometers a hybrid solution was established. In this case the raw cADCS magnetometer readings as well as a derived cADCS sun vector are sent to the iADCS as sensor
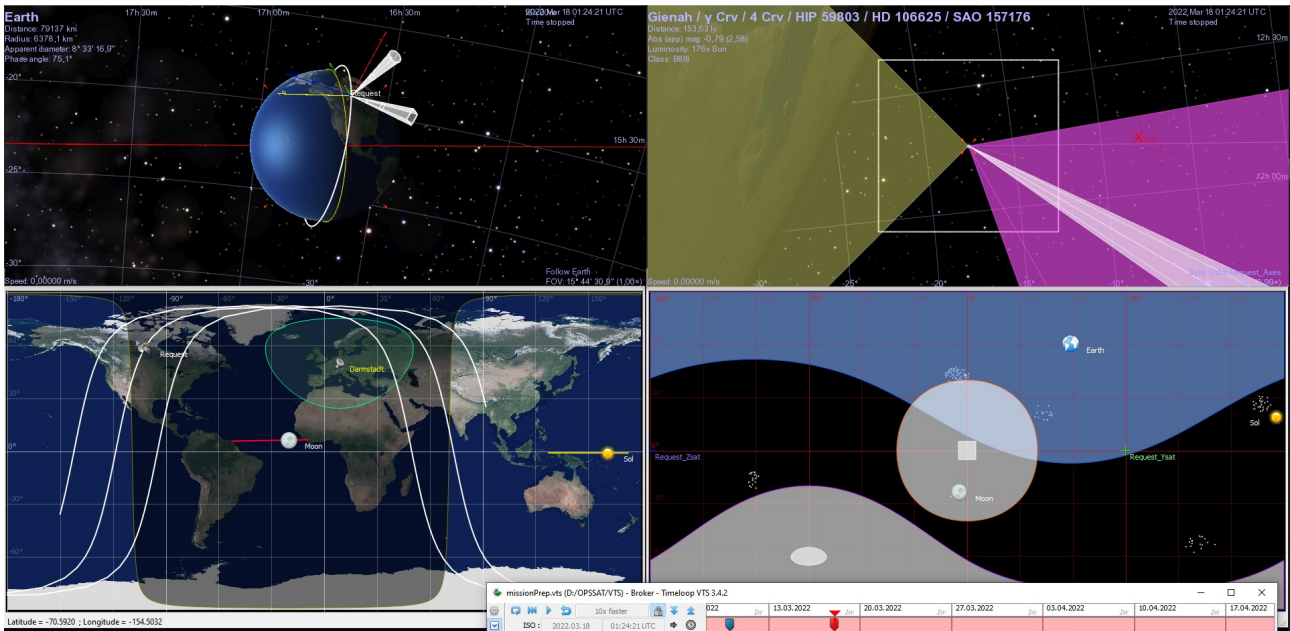

Figure 3: Here, the target is the star Gienah, m_V=2.58, in the Corvu constellation. OPS-SAT's orientation in mission preparation must ensure that the Earth, the Moon and the Sun will not illuminate the Star Tracker (circular cone) or the Imager (square cone). CNES' free software VTS is used to check the decided quaternion.

inputs. The iADCS uses these inputs until it establishes a good attitude in which star tracker measurements can be relied on. This improved the situation but it did not work all the time and the ESA team were faced with a challenge of how to improve the system without any ground truth, i.e. a sensor measurement one could rely on when there was no star tracker values available.

This issue at inertial pointing was known when we submitted an astrometry algorithm labelled "AbC" on OPS-SAT. It was approved as an OPS-SAT experiment on 21st Dec 2020. The experiment aims at imaging various known star-fields and characterizing the field of view in details. Eventually, it shall assess the efficiency of the AbC algorithm. Due to the existing feed-back on OPS-SAT's stability with iADCS-100 and, reversely, the lack of feed-back at imaging stars with IMS-100, it was decided to use the astrometry techniques to characterize the ADCS itself on the basis of a deep analysis of images of the sky. When the inertial pointing is fully stabilized, the original AbC will be implemented for OPS-SAT and hopefully uploaded and run in space. In the meantime, the images taken for ADCS characterization will serve as a database to test the AbC on ground.

2.2   Operations for ADCS characterization

The operations for this experiment follow a trial and error process between CENSUS (experimenter team at Paris Observatory) and OPS-SAT (ESA operators).

CENSUS computes a quaternion, for the weeks to come, that targets an area in the anti-solar hemisphere with multiple bright stars and allowing the -X panel to be illuminated by the Sun. The rotation about the wanted bore-sight is decided to avoid the illumination of the star tracker by the Sun. Then, the best periods along the orbit to perform pictures are indicated to make sure that the imager and the star tracker are not occulted by the Earth or illuminated by its dayside. Computations are checked in displays provided by VTS (example in Fig. 3), a free software that is specialized for space operations, developed by the French space agency CNES .

Then, the OPS-SAT team plans the inertial pointing and the capture of images with the provided quaternion in the best way possible, along with all experiments to be run. The inertial pointing
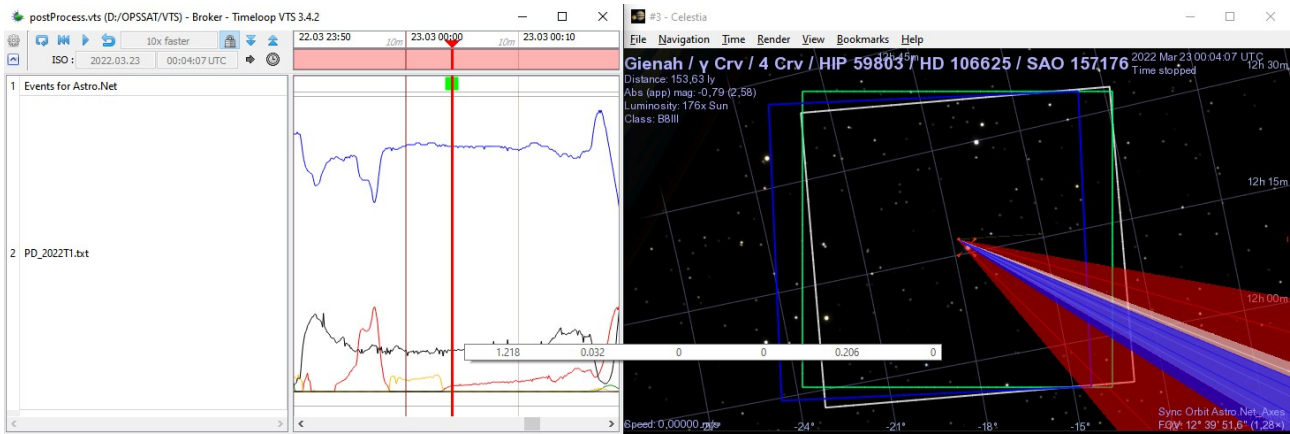
Figure 4: Trial on March 23, 2022. Actual field of view as reconstructed from the pictures (green square), with the requested (white) and the on-board estimated (blue) orientations. Star tracker is orientated to the bottom right. Chronograms of the photodiodes are displayed on the left panel (PD1, PD2 and PD5 are illuminated, see Fig. 10).

operations consist of a sequence of commands to initialize iADCS, enable telemetry, send magnetometer and sun state vectors to iADCS, start the pointing operation with desired quaternions as input. After the first characterizations of stars, we decided to capture series of 5 images in a row, that we call a "burst", each image with a 500-ms exposure time, covering 2.5 s per burst. One image weighs 7.8-MB in raw format. The images are timestamped with the on-board clock, whose drift from the CPU time is reset daily and kept lower than ~1 s. The images are downloaded to the ground station, then deposited in a folder shared with CENSUS.

The images are processed by CENSUS with manual validations at various steps of the process. First, the cosmic rays above the brightest star signal are removed and cataloged for every image. The cleaned images are saved as a compressed PNG image (between 500 and 1500 KB in size). Then, each area with a candidate star is displayed and a manual decision is made whether or not it is classified as a star. For a burst of 5 successfully processed images, the cleaned images are re-aligned on the two brightest stars identified and stacked. The resulting image is submitted to the open-source Internet free service "Astrometry.net" [3], which returns a full characterization of the field of view if successful, that is, then, translated into an equivalent OPS-SAT quaternion. The telemetry of the ADCS and the photo diodes are also retrieved from OPS-SAT server. The whole data is formatted to get displayed in VTS and to compare the requested, the reached and the on-board estimated orientations. The example given in Figure 4 was obtained on March 23, 2022 and shows less than 0.5° between the 3 orientations.

Eventually, reports are written for the bursts that could be successfully processed. They are discussed between CENSUS and OPS-SAT to consider improvements in the operations, in the systems and in the processing.

2.3   Initial Results: star detection

We first took images to identify an efficient exposure time. Images of the Earth dayside surface require as short as 2 ms. A series of images was taken from October 18, 2021 with exposure times of 2, 15, 50, 100, 120, 500 and 800 ms. With 500 ms, the same pattern of 3 stars was visible in different pictures without complex post processing. From these first images, we could make some initial assessments:

- an important number of pixels (several hundreds) dominate the signal in the pictures, well above the signal received from stars, preventing a direct search for star signal areas;

- a large part of these "high" pixels are "hot" pixels, i.e. same pixels in all images at high
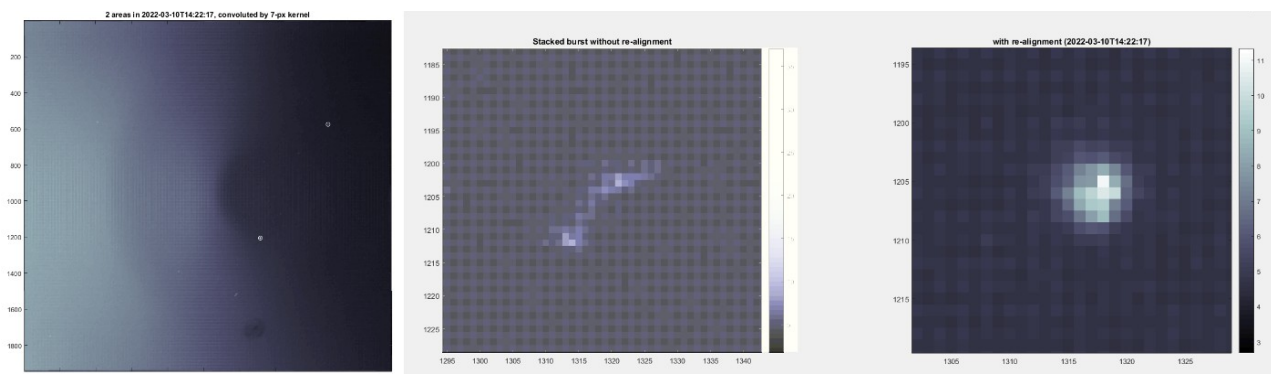

Figure 5: Image taken on 2022-03-10 with some straylight. Left: 2 stars are seen (circles) along with a distortion pattern. Stacked images of a star, without re-alignment (center, contrast enhanced) and with re-alignment (right).
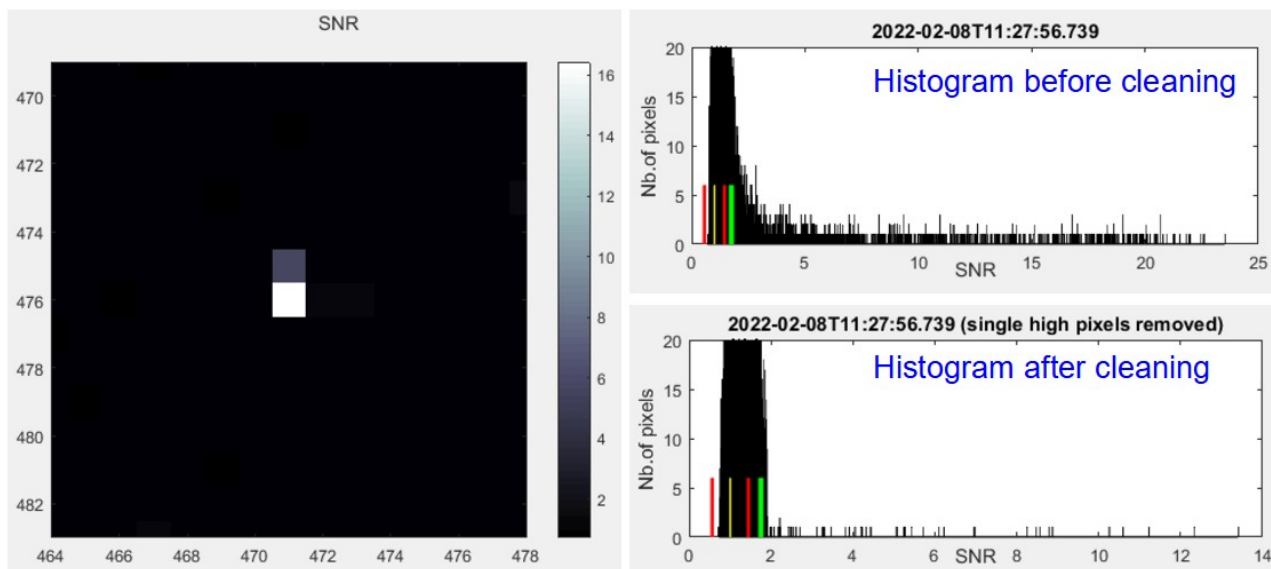

Figure 6: Cosmic rays removal. Left: cosmic that spreaded on multiple adjacent pixels (SNR 16). Right: histogram (normalized on SNR) with all pixels up to SNR 24 (top) and without cosmics up to SNR 13.5 (bottom).

level, they are believed to be permanently damaged by cosmic rays;

- in areas where stars can be seen, the light is spread over areas from 7×7 to 10×10 pixels, meaning that only a very small fraction of the star light (typically 1/50th) is captured by one single pixel and resulting in very dim star images, while the PSF is expected smaller than a pixel (550 nm with a 2 cm lens yields a 5.7 arcsec PSF, while pixel size is 18 arcsec);

- instability of the platform make 800 ms exposure times worse than 500 ms which was selected as the best compromise;

- on some images with stray-light, the focal plane appears strongly distorted, with a permanent pattern that would likely bias any analysis based on level variations of the signal (whether this could be compensated with an updated PRNU[1] calibration has not been studied so far).

With an exposure time at 500 ms, a setup was developed to take series of 5 images in a row, called bursts. It was then possible to detect at least two stars in each of the 5 pictures of a given burst, allowing the re-alignment of all 5 images of the burst to, eventually, stack the images. An example of the stacked images is given in Figure 5: the two main stars are circled in white (left), stray-light is seen entering from the left, the 5 images of the main star are stacked without re-alignment

---

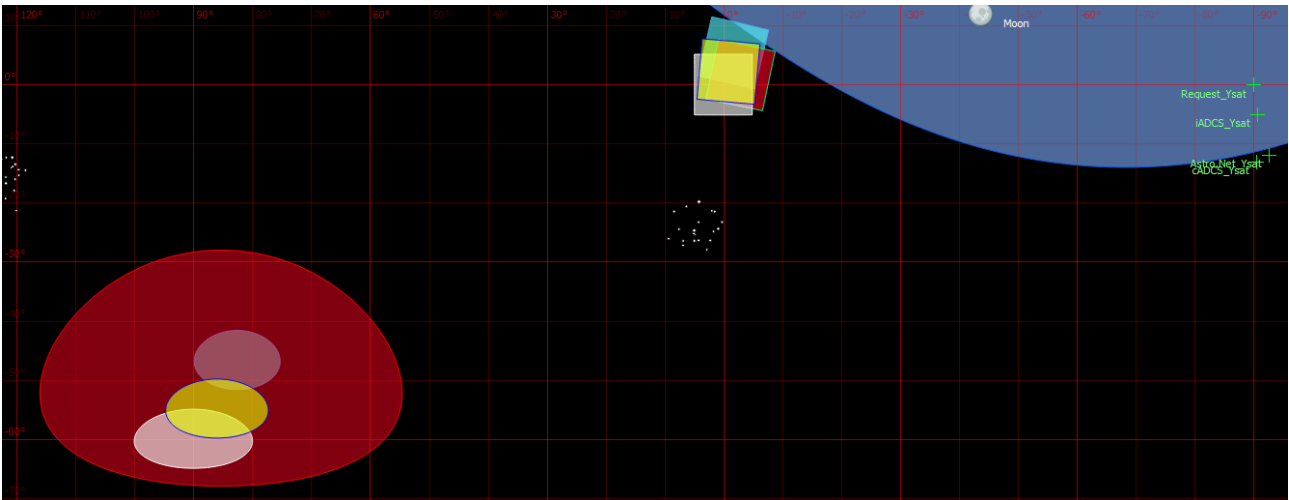1   PRNU - Photon Response Non Uniformity

Figure 7: Synthetic view in VTS, reconstructed for 2022-03-22T08:15:11 burst. Squares: Imager field of view as requested (white), reconstructed by Astrometry.net (red), estimated by iADCS (green, behind red) and by cADCS (light blue), corresponding $+Y_{SAT}$ axes (green, right). Ovales indicate the corresponding directions of the star tracker.

(center) and with re-alignment (right). When successfully stacking without straylight, more than 20 stars are often revealed and these stars are later confirmed by Astrometry.net with only few wrong detections.

The image processing starts with the removal of high/hot pixels, that reveals stars and, eventually, allows the image to be submitted to Astrometry.net. Once the image is decoded, the red, green and blue channels are normalized: the medians for each color are extracted from all pixels of the color and pixels of a color are divided by the median of that color, yielding a scale in monochromatic Signal-to-Noise Ratio (SNR) units. Of course, as a result, a blue star (for instance) would be strongly mosaiced but this is preferred to an interpolation of the RGGB Bayer pattern that will spread the hot pixels into false star images. Then, all isolated high pixels are deemed "potentially hot" and registered. They were later analyzed on the basis of the first 36 images and an initial list of 1016 permanently hot pixels was extracted. This list could be updated and uploaded in the satellite if on-board cleaning is wanted in the future. The effect of cleaning is clearly seen in the histograms of Figure 6: the pixels beyond the green bar contain signal above SNR+5.1 σ, which corresponds to a probability lower than 1 over 4 millions (number of pixels) to have Gaussian noise that high in a pixel. After the cleaning process, only a few tens of pixels remain above SNR+5.1 σ and are deemed to contain a physical signal that is not due to cosmic rays.

Unfortunately, cosmic rays can fill several adjacent pixels, as shown in Fig. 6 (left), for instance if they hit the sensor tangentially. The automatic removal process can no longer apply in such cases. Then, they will be manually ignored in the processing when examining the star candidates.

2.4 Image-based characterization

The characterization, still on-going at the time of writing, has targeted first order discrepancies in the pointing and stability. It reconstructs the actual attitude on the basis of the identification of imaged star-fields and the comparisons with the commanded and the on-board estimated attitude.

The cleaning of an image is essential to search for star candidates. Other tasks should also be performed but they are not critical to stack and assess the imaged region of the sky: hence, DCNU[2] and PRNU adjustments (as given by the manufacturer after IMS-100 ground calibration) as well as corrections of the optical aberrations have not been performed yet. Nevertheless, DCNU and PRNU

---

2   DSNU - Dark Signal Non-Uniformity

that would include a correction of the distortions reported in Fig. 5, will help the star identification and the management of stray light, which is still a concern. Also, astrometry reduction would require a thorough correction of the optical aberrations: it was noticed that expected stars are several pixels away from their expected location when they are close to the edge of the image (the detailed analysis was not available at the time of writing).

After an initial period of trials and errors, multiple bursts were successful from January 2022, meaning that they allowed a successful stacking of the 5 elementary images, a successful match with Astrometry.net along with a pointing in close proximity to the request. Table 1 lists the first 7 successful bursts from January to March 2022. The offsets are reported with the accuracy of a 10th of a degree for the boresight and one degree for the rotations, due to the manual reading of the directions (an example is provided in Fig. 7 for the burst "E" of Table 1) and the precision of Astrometry.net reduction.

The star tracker was used for the pointing in all observations but "A". End of January, a BST suggested change was uploaded to modify some configuration parameters in the iADCS Kalman filter. Apart from the reported list, it must be noted that multiple attempts were performed with two more quaternions (not reported here) specified for the periods from mid-January to mid-March 2022 but they could not produce any close pointing from the request or stabilized pointing, and the reasons are still unclear.

#	Timestamp	Target (Long, Lat) ICRF	Astrometry.net match (offset)	iADCS estimate (offset)	cADCS estimate (offset)
A	2022-01-13T11:49:20	(101.287, -16.716)	(+3.3;-6.6) rot.-13°	(+0.2;-1.1) rot.-2°	(+1.5;-5.1) rot.-14°
B	2022-01-20T13:08:55	(101.287, -16.716)	(+3.1;-4.3) rot.-4°	(+0.5;-2.0) rot.-3°	(+2.7;-3.0) rot.-6°
C	2022-01-21T14:28:04	(101.287, -16.716)	(+3.2;-4.1) rot.-3°	(+0.2;-1.3) rot.-2°	(+1.4;-2.2) rot.-4°
D	2022-03-10T14:22:17	(47.267, +49.613)	(+2.1;+1.1) rot.-5°	(+0.4;-0.6) rot.-1°	(+2.7;-2.2) rot.-4°
E	2022-03-22T08:15:11	(183.952, -17.542)	(+2.9;-1.6) rot.-12°	(+0.9;-2.2) rot.-5°	(+1.7;-5.4) rot.-13°
F	2022-03-22T20:54:22	(183.952, -17.542)	(-1.5;-1.3) rot.-5°	(-0.1;-0.6) rot.-1°	(+0.4;-2.6) rot.-5°
G	2022-03-23T00:04:08	(183.952, -17.542)	(+0.3;-0.3) rot.-5°	(+0.2;-1.2) rot.-2°	(-0.8;-2.8) rot.-5°

Table 1: List of first 7 successful bursts. Offsets from Target are expressed in (Az.;Elev.)[degree] of the boresight in (+Y/Az.; +X/Elev.) satellite axes, and rotation about +Z[degree]. Quaternions are given in Appendix.

In addition of the reported offsets, a deeper analysis of the telemetry shows that the iADCS estimate converges to the request (Target) and keeps a constant offset with it between 0.5° and 1°. However, the actual field of view is distant from the request by a larger angle. This suggest that there is a misalignment of the star tracker and a larger misalignment of the imager. The installation of the star tracker and the imager on OPS-SAT is specified by fixed quaternions q_{FoV} and q_{ST} that transform the satellite body frame into their respective frames:

$$q_{FoV} = 0 + \vec{v}[1,0,0]$$
$$q_{ST} = 0.683 + \vec{v}[0.183, 0.683, -0.183] \tag{1}$$

However, due to various factors like the integration on ground, the launch or the possible thermal stress in orbit, these quaternions may have become inaccurate. The imager's field of view is the only ground-truth verification while all transforms assume fixed quaternions q_{FoV}, q_{ST} and also for the Sun sensor. Hence, based on these results, a search for adjusted quaternions q'_{FoV} and q'_{ST} that would best fit the observed images is possible and was just starting at the time of writing.

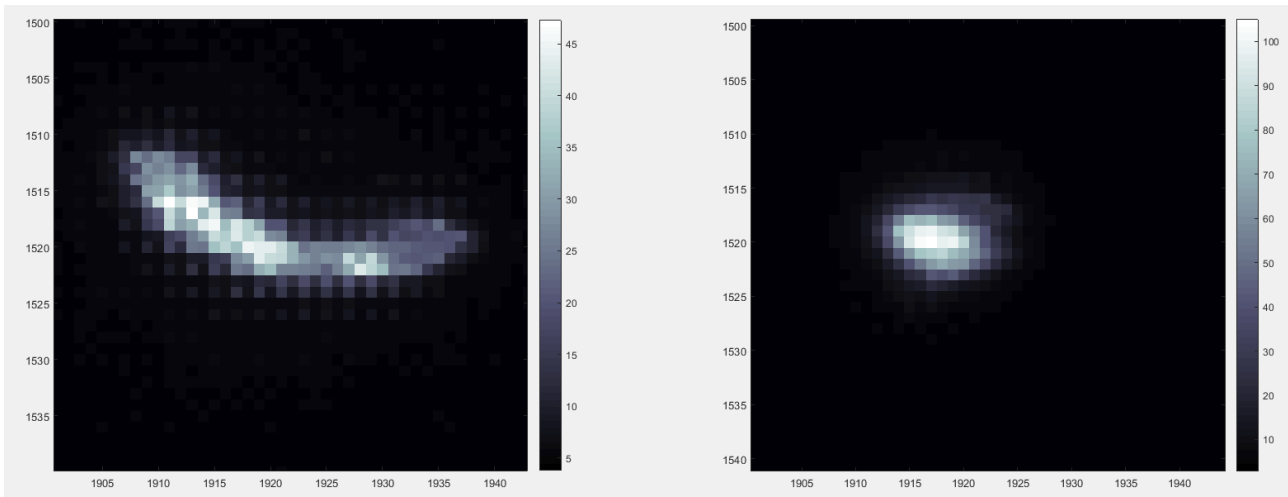Another major hint of the images is the assessment of the stability. The stacked of 5 × 0.5 s images

Figure 8: 5 stacked images of Sirius during the observation "B", without (left) and with (right) re-alignment. Total exposure time: 5 × 0.5 s

without re-alignment reveals the platform motion over 2.5 s (Fig. 8). The track expands along the X-axis of the non re-aligned image over 30 pixels, with an average size of 10 pixels as it can be seen on the re-aligned image, meaning that a first-order of the motion is 20 pixels over 2.5 s, i.e. a drift of ~0,04°/s (the pixel size is 18"). The presented burst is for observation "B" and was fairly stable. More generally, the drift is reported on successful stacked images up to 0.08°/s. The stacked image of a star shows the average motion at frequencies higher than 2 Hz (0.5 s) but it is not possible to tell whether it results from jitter like vibrations due to reaction wheels or wobbling due to the ADCS control laws (e.g. from B-dot magnet-torques). However, a more detailed analysis could be considered with shorter exposure times and reliable pointing to known bright stars.

Eventually, the submission of cleaned images to Astrometry.net provides a characterization of the sensor geometry itself: sensor's angular size and best fit of distortion coefficients. In the case of the IMS-100 on OPS-SAT, the measured field of view is assessed at 10.3° × 9,81° with an average pixel size of 18.1 arcsec. Astrometry.net computes the distortion coefficients in the Simple Imaging Polynomial (SIP) convention [4]. The use of this set of coefficients in OPS-SAT context is still a work to do, together with techniques to search an area of interest and to measure the photocenters. As an insight, a plot of the matched stars in the submitted image and in Astrometry.net's catalog, after fine rotation alignment, shows substantial radial distortions (Fig. 9) that shall not be ignored in astrometry processing.

3   LESSONS LEARNED

It is very difficult to troubleshoot ADCS problems without some sort of ground truth assessment. Magnetometer measurements are only as good as the model they compare against and they are influenced by the on-board magnetic field, especially on cubesats. Gyros do not provide absolute measurements and are influenced by temperature and sun sensors/photo diodes have to be calibrated correctly at all different angles if they are to be trusted. Star trackers are the closest we come to ground truth but even they can be misaligned. In this mission we found that pictures of the stars taken from the platform provided that ground-truth assessment of the imager's orientation and, consequently, of the platform's resilience and behavior in the space environment.

3.1   In-flight characterization

The images taken with the standard camera on-board a 3-Unit CubeSat have allowed to assess the exact pointing of the imager with an accuracy of 0.1° degree for the boresight in a first analysis, and
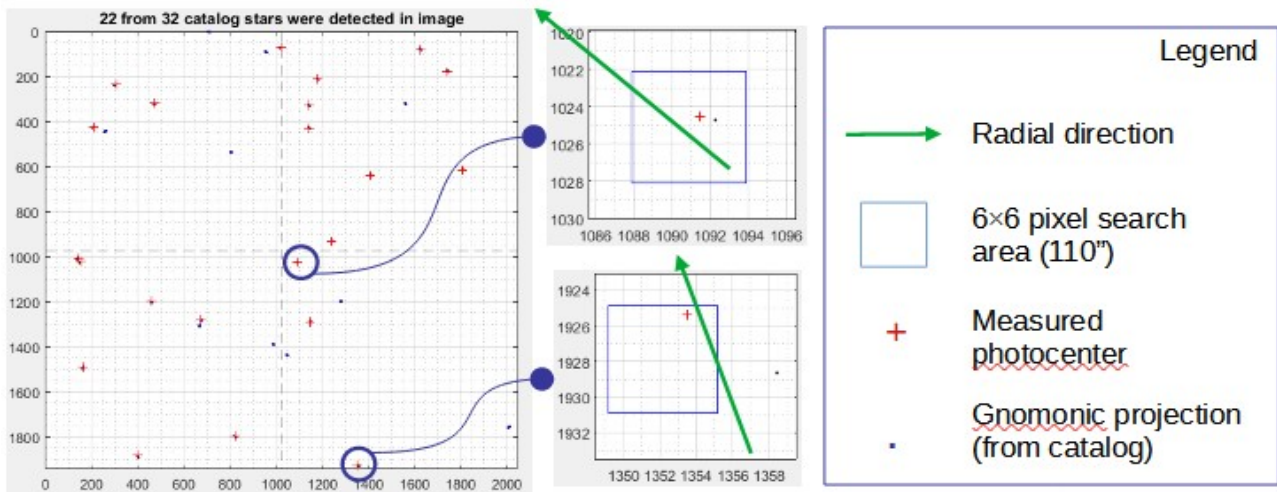
Figure 9: Distortions in the observation "G": in the radial direction, ~1 px for a star close to the center (top right), ~6 px for a star close to the edge (bottom right, gnomonic projection to the right of the square area).

the accuracy will be improved with a deeper astrometry reduction of the fields of views.

Then, the dynamic of the on-board estimated quaternions of the iADCS, just before and after the image, suggests two different alignment errors: one for the star tracker itself that can be seen in the difference between the request and the iADCS estimate, and one for the imager in the difference between the iADCS estimate and the actual imager's orientation. After a re-alignment correction, it will be possible to assess the possible misalignment of the Sun sensor as well.

The stability of the platform was also quantified from the images: tracks of stars are mainly associated with a drift of 0.04°/s to 0.08°/s. The jitter at frequencies higher than 2 Hz was not measured (it remains within 5 pixels = 90 arcsec), but its quantification could be improved with dedicated stable pointing and exposure time shorter than 0.5 s.

The sensor of IMS-100 was characterized precisely with an independent database, Astrometry.net, in terms of geometry and main distortion coefficients. The analysis of the hot pixels provide a clear assessment of the aging and a good feedback to specify the shielding for future nanosatellites. In addition, single star images extracted from tens of images have populated a database. The possible statistics can serve to specify the sensitivity of the IMS-100, considering the stability of the platform and the use of an RGGB Bayer pattern, usually not expected for astrometry purpose.

3.2 Ground testing and commissioning

CubeSat hardware is not expected to offer the same stability and sensitivity compared to hardware for larger space missions. Whatever the performances, they must be reliable to reach a proper design. The NewSpace paradigm is to rely on COTS, to fly an experiment (at lower costs), to gain experience and to refly. Nevertheless, each CubeSat is different and designed to reach performances for the overall functional chains, integrating multiple COTS.

OPS-SAT offers to test new techniques and algorithms in operations. It has proved its flexibility, including for our astrometry experiment that is interesting for OPS-SAT itself. We were able to engage, a posteriori, into a deep analysis of the ADCS. The set up of the ground segment (mission preparation, operations and post processing) took about 6 months and involved 7+ engineers of Paris Observatory and ESA, at various levels, with the support of BST. In the particular case of OPS-SAT, the lack of a priori knowledge about images of stars forced us to trials in flight. In a general case, where an image-based commissioning can be anticipated, the ground segment can get prepared well before launch with an optical bench and some setup to mimic drift, vibrations and

straylight on the imager and the star tracker. The interest is to check the exclusion angles, the sensitivity and, later, to commission these performances in flight.

The commissioning of the systems in traditional space missions is an important milestone, technically and contractually. It comes with a set of more or less complex operations. For some reasons, the operations for nanosatellites in the NewSpace commonly do not anticipate extensive procedures if the integrated systems do not work properly. It is not specific to any particular nanosatellite whose COTS are provided "as is" (by definition). Likely the "hope" of reliability of the COTS, as claimed by the manufacturers, and the pressure of the launch planning, explains some risky shortcuts in the integration tests. Also, the difficulty to set up tests on ground that could mimic the conditions in space, especially for ADCS, results in a lack of experience at stimulating the full functional chains, once integrated, and possibly in a lack of diagnostic and troubleshooting procedures in flight. The traditional space missions, that cannot test entirely the ADCS either, rely on a thorough combination of elementary tests and control law simulations and, then, on in-flight parameters and redundancy that can be adapted to actual performances measured after launch.

For sure, the test of ADCS is a complicated task. And even the simplest CubeSat has to integrate a full set of sensors and actuators whose calibrations depend on many factors of the flight domain (e.g. thermal stress, alignments, aging). Their combination in flight cannot be anticipated and absolute measurements are needed. That is what image-based analysis can provide. The simplest approach is to anticipate the update of alignment parameters after launch. A more complex approach is to simulate misalignment during ground tests and define diagnostic procedures to update the alignments.

3.3   Specifications

Specifications can be expressed at the procurement stage but, in the NewSpace, the customer takes what is available. Nevertheless, an important part of the technical performance and of the NewSpace value chain is at the integration level, with many new providers, and allows new types of relationships.

System budget margins must be saved for the integration and "managed" with the integrator. For a project that would have similar concerns like OPS-SAT (likely all nanosatellites), the following performances could be specified beforehand and verified with image-based astrometry:

- based on the inertial momentum matrix, maximum duration to stabilize drift & jitter

- sensitivity of the gyrometers

- accuracy / convergence of the on-board attitude estimators

- sensitivity and exclusion angles of the sensors

- resilience of the imager with the cosmic rays

In coherence with the NewSpace paradigm, some success fees should certainly be negotiated at the COTS manufacturer level (resilience, sensitivities, exclusion angles) and at the integrator level (drift & jitter, reflections on the structure, estimators). A common approach in space engineering is to specify the performances as a "goal" vs. a "target", to express two levels of system budget margins. These same levels could be the basis for a success-fee lever in the NewSpace. For sure, an arbitration must be available to assess the truth and this can be the image-based astrometry.

4   CONCLUSIONS

In this paper, we presented some results of a successful attempt to perform image-based astrometry

from the 3-Unit CubeSat OPS-SAT. Although the experiment is still on-going, it was possible to image stars with a COTS imager and to get their identification from the on-line free service Astrometry.net, along with a detailed characterization of the field of view captured by the device.

A thorough processing of the pictures yields the quantification of the stability of the platform in various operational setups and how it became an integral part of the efforts to improve operations and to troubleshoot the "inertial pointing" high-level ADCS mode of the satellite. Work is still on-going to assess new alignment parameters of the various sensors on board (star tracker, imager, Sun sensor) as they appear to be different from the specification.

The images of stars and their surrounding noise provide insights on the resilience of the sensor with the cosmic rays. They give an access to the in-flight optical distortions and the sensitivity with an RGGB Bayer pattern. Some images with straylight can serve as a basis to update the PRNU.

The improvements on the pointing and the knowledge on the sensor allow the development of a novel astrometry technique at CubeSat scale. The lessons learned here also inspire ground tests and a full commissioning process of the ADCS. We also suggest ways to specify and to subcontract subsystems and their integration on nanosatellites to improve performances in flight.

5   ACKNOWLEDGMENTS

6   REFERENCES

[1] D. Evans and A. Lange, "OPS-SAT: Operational concept for ESA'S first mission dedicated to operational technology," SpaceOps 2016 Conf., no. January, 2016.

[2] G. Labrèche, D. Evans, D. Marszk, T. Mladenov, V. Shiradhonkar, V. Zelenevskiy, "Agile Development and Rapid Prototyping in a Flying Mission with Open Source Software Reuse On-Board the OPS-SAT Spacecraft," AIAA SCITECH 2022 Forum, DOI 10.2514/6.2022-0648

[3] D. Lang, D. W. Hogg, K. Mierle, M. Blanton, and S. Roweis, "Astrometry.net: Blind astrometric calibration of arbitrary astronomical images," Astron. J., vol. 139, no. 5, pp. 1782–1800, 2010.

[4] D. L. Shupe, M. Moshir, J. Li, D. Makovoz, and R. N. Hook, "The SIP Convention for Representing Distortion in FITS Image Headers," Astron. Data Anal. Softw. Syst. XIV ASP Conf. Ser. Vol. XXX, 2005, vol. 347, p. 491, 2005.

[5] CNES, "VTS, Visualization Too for Space data", available at https://timeloop.fr/vts, Centre National d'Etudes Spatiales.

[6] SIMBAD database, operated at CDS, Strasbourg, France, https://simbad.u-strasbg.fr/simbad/

7   APPENDIX

7.1   Location of the Photodiodes

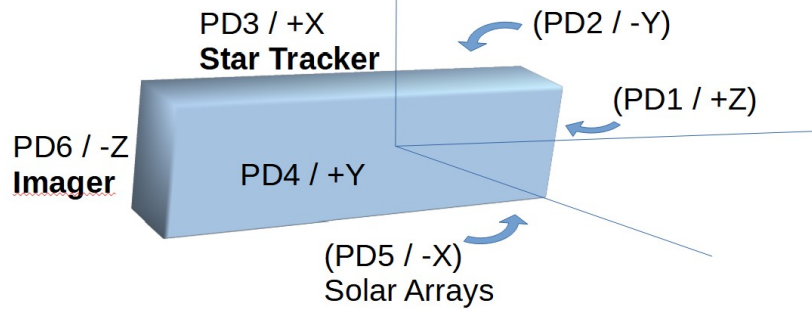|		
CADC0884	I_PD1_THETA	Z+
CADC0886	I_PD2_THETA	Y-
CADC0888	I_PD3_THETA	X+
CADC0890	I_PD4_THETA	Y+
CADC0892	I_PD5_THETA	X-
CADC0894	I_PD6_THETA	Z-

Figure 10: Location of the Photodiodes on OPS-SAT sides

7.2   Measured and estimated quaternions

#	Timestamp	Requested quaternion	Actual quaternion
A	2022-01-13T11:49:20	s(-0.4058) + v[-0.3433, 0.4230, -0.7338]	s(-0.4058) + v[-0.3433, 0.4230, -0.7338]
B	2022-01-20T13:08:55	s(-0.2987) + v[-0.3263, 0.4997, -0.7447]	s(-0.3352) + v[-0.3219, 0.4572, -0.7583]
C	2022-01-21T14:28:04	s(-0.2987) + v[-0.3263, 0.4997, -0.7447]	s(-0.3269) + v[-0.3192, 0.4599, -0.7614]
D	2022-03-10T14:22:17	s(0.1983) + v[-0.1294, -0.9295, 0.2827]	s(0.2051) + v[-0.0821, -0.9304, 0.2924]
E	2022-03-22T08:15:11	s(0.0221) + v[0.5883, 0.0569, 0.8064]	s(-0.0905) + v[-0.5661, -0.1371, -0.8078]
F	2022-03-22T20:54:22	s(0.0221) + v[0.5883, 0.0569, 0.8064]	s(-0.0670) + v[-0.5756, -0.0735, -0.8116]
G	2022-03-23T00:04:08	s(0.0221) + v[0.5883, 0.0569, 0.8064]	s(-0.0543) + v[-0.5831, -0.0835, -0.8062]

Table 2: List of quaternions for the 7 first successful bursts: Requested in mission preparation and Actual as reconstructed from Astrometry.net. Quaternions are expressed as the transform of the satellite body frame from ICRF to the pointing, using CNES' VTS convention, under the form (scalar)+[vector].

#	Timestamp	iADCS quaternion	cADCS quaternion
A	2022-01-13T11:49:20	s(0.3164) + v[0.3273, -0.4893, 0.7437]	s(-0.4110) + v[-0.3518, 0.4345, -0.7200]
B	2022-01-20T13:08:55	s(-0.3287) + v[-0.3293, 0.4813, -0.7427]	s(0.3459) + v[0.3393, -0.4562, 0.7463]
C	2022-01-21T14:28:04	s(-0.3179) + v[-0.3276, 0.4889, -0.7432]	s(0.3325) + v[0.3340, -0.4727, 0.7445]
D	2022-03-10T14:22:17	s(-0.2051) + v[0.1236, 0.9286, -0.2832]	s(0.2288) + v[-0.1001, -0.9224, 0.2944]
E	2022-03-22T08:15:11	s(-0.0583) + v[-0.5654, -0.0947, -0.8172]	s(-0.1041) + v[-0.5390, -0.1309, -0.8254]
F	2022-03-22T20:54:22	s(-0.0315) + v[-0.5835, -0.0624, -0.8090]	s(0.0548) + v[0.5662, 0.0851, 0.8180]
G	2022-03-23T00:04:08	s(-0.0365) + v[-0.5784, -0.0695, -0.8119]	s(-0.0622) + v[-0.5645, -0.0768, -0.8194]

Table 3: List of on-board estimates of the quaternions for the 7 first successful bursts: estimated by iADCS and cADCS. Quaternions are expressed as the transform of the satellite body frame from ICRF to the pointing, using CNES' VTS convention, under the form (scalar)+[vector].